Sharpening vision by adapting to flicker

Derek H. Arnold[a,1], Jeremy D. Williams[a], Natasha E. Phipps[a], and Melvyn A. Goodale[b]

[a]Perception Laboratory, School of Psychology, University of Queensland, Brisbane, QLD 4072, Australia; and [b]Brain and Mind Institute, Western University, London, ON N6A 5B8, Canada

Edited by Randolph Blake, Vanderbilt University, Nashville, TN, and approved August 31, 2016 (received for review June 12, 2016)

Human vision is surprisingly malleable. A static stimulus can seem to move after prolonged exposure to movement (the motion aftereffect), and exposure to tilted lines can make vertical lines seem oppositely tilted (the tilt aftereffect). The paradigm used to induce such distortions (adaptation) can provide powerful insights into the computations underlying human visual experience. Previously spatial form and stimulus dynamics were thought to be encoded independently, but here we show that adaptation to stimulus dynamics can sharpen form perception. We find that fast flicker adaptation (FFAd) shifts the tuning of face perception to higher spatial frequencies, enhances the acuity of spatial vision—allowing people to localize inputs with greater precision and to read finer scaled text, and it selectively reduces sensitivity to coarse-scale form signals. These findings are consistent with two interrelated influences: FFAd reduces the responsiveness of magnocellular neurons (which are important for encoding dynamics, but can have poor spatial resolution), and magnocellular responses contribute coarse spatial scale information when the visual system synthesizes form signals. Consequently, when magnocellular responses are mitigated via FFAd, human form perception is transiently sharpened because "blur" signals are mitigated.

spatial vision | adaptation | visual acuity | flicker

Analyses of form and of stimulus dynamics within human vision were thought to be independent (1–3), but later evidence has challenged a strict division. Many brain regions contain large numbers of neurons responsive to both spatial form and to movement (4–6), and it has been demonstrated that human vision can generate direction-tuned representations of form (7). These observations do not, however, dictate that visual analyses are undifferentiated. Rather, the nature of specialization might be more nuanced than previously appreciated.

Separate visual pathways have been identified, and these appear to have diverging patterns of spatiotemporal sensitivity. Some mechanisms, often referred to as "magnocellular," integrate information from across relatively large retinal regions, but only small expanses of time (8–10). Due to their high temporal resolution, these spatially low-pass, temporally band-pass mechanisms are well suited for encoding information about stimulus dynamics and fast moving form, but they are insensitive to fine spatial detail (11). Such mechanisms could be disproportionately concentrated in dorsal pathway brain structures (12). Other mechanisms, often referred to as "parvocellular," integrate information from across smaller retinal expanses and more extended expanses of time (13, 14). Due to their higher spatial resolution, these spatially band-pass, temporally low-pass mechanisms are well suited for encoding information about fine spatial detail, but due to their protracted integration times (~100 ms, see ref. 15) they encode fast moving form as blur (10, 11, 16).

Consistent with a spatiotemporal-based specialization, one study showed that exposure to a rapidly moving form containing fine spatial detail can induce human vision to generate conflicting illusory form signals that compete for perceptual dominance (17). One was an impression of a rapidly moving form devoid of fine spatial detail. The other was of a blurred static form, with fine spatial detail but no apparent movement. This shows that diverse mechanisms in human vision can generate independent conflicting form signals when exposed to a common input, but in normal circumstances, these mechanisms probably combine to support coherent impressions of form (7). Alternatively, it is possible that perceptual experience is usually dominated by a subset of spatiotemporal mechanisms, and that signals from other mechanisms are suppressed—or masked—from awareness (18, 19).

We can assess these possibilities by transiently reducing the contribution of one of these two broad classes of spatiotemporal mechanism via adaptation—by persistent exposure to a stimulus that better matches the response characteristics of one of the two classes of mechanism. For this adaptation, we will use dynamic noise, which excites a robust response from spatially low-pass, temporally band-pass mechanisms, but little from spatially band-pass, temporally low-pass mechanisms (as dynamic noise sums to gray over small expanses of time). We refer to this as fast flicker adaptation (FFAd). Our central question thus reduces to the following: What, if any, impact will FFAd have on spatial form perception? As dynamic white noise induces little response from mechanisms optimized for encoding spatial form, one might suppose this adaptation will have no impact. We, however, suggest that "magno" fed mechanisms usually contribute coarse spatial scale information when human vision synthesizes form signals. Mitigating this contribution via FFAd will therefore sharpen spatial vision, by exaggerating the contribution of unadapted mechanisms that encode finer spatial detail.

In experiment 1, we assess whether FFAd can have a perceptual impact on the encoding of what is perhaps the most important ecological form for humans—the human face. It is possible to generate hybrid images that depict two different faces in different spatial frequency bands (20). Fig. 1*A* is an array of such images. At either end of the array a single face is depicted. On the far left the face is blurred (low-pass filtered in the spatial frequency domain) and on the far right, sharpened (band-pass filtered in the spatial frequency domain). In between images are mixed, with contrasts of the two components oppositely linearly modulated, balanced in the middle. Looking across the array one can see a blurred feminine face gradually transform into a sharpened masculine face.

Significance

Distinct anatomical visual pathways can be traced through the human central nervous system. These have been linked to specialized functions, such as encoding information about spatial forms (like the human face and text) and stimulus dynamics (flicker or movement). Our experiments are inconsistent with this strict division. They show that mechanisms responsive to flicker can alter form perception, with vision transiently sharpened by weakening the influence of flicker-sensitive mechanisms by prolonged exposure to flicker. So, next time you are trying to read fine print, you might be well advised to first view a flickering stimulus!

Author contributions: D.H.A., J.D.W., and M.A.G. designed research; D.H.A., J.D.W., and N.E.P. performed research; D.H.A. and J.D.W. analyzed data; and D.H.A., J.D.W., and M.A.G. wrote the paper.

The authors declare no conflict of interest.

This article is a PNAS Direct Submission.

[1]To whom correspondence should be addressed. Email: d.arnold@psy.uq.edu.au.

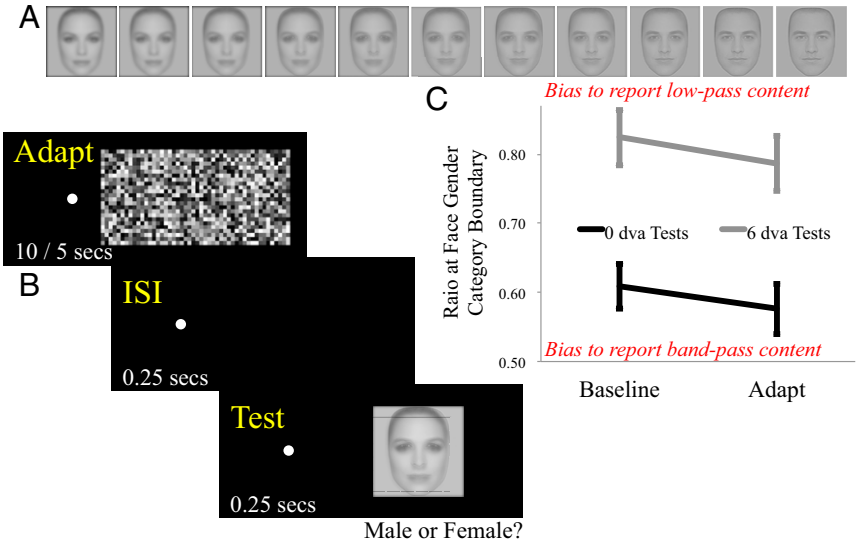

Fig. 1. (*A*) Depiction of an array of test images used in experiment 1. One of the two arrays ranged between a low-pass filtered female face and a band-pass filtered male face (as depicted here); the other ranged between a low-pass filtered male face and a band-pass filtered female face (see main text for further details). (*B*) Depiction of trial sequence during an adaptation block of trials. (*C*) Low-pass to band-pass image content ratios corresponding to gender face category boundaries as a function of adaptation (baseline/adapted) and test eccentricity (0/6 dva). Higher values indicate a greater bias to report the facial gender signaled by low-pass image content, and lower values signify a tendency to report the facial gender signaled by band-pass image content. Error bars depict ±1 SEM.

Facial appearance in hybrid images depends on the dominant band of spatial frequencies. One way to modulate the facial appearance of hybrid images is to increase (or decrease) viewing distance, as this shifts the facial image toward higher (or lower) retinal spatial frequencies, by reducing (or increasing) the size of the image on the retinae. Another way is to shift images into the periphery of vision, as human sensitivity to high spatial frequencies diminishes with increasing distance from fixation. Readers should find they can modulate the appearance of midarray images in Fig. 1*A*, in terms of gender, via either manipulation. In experiment 1, we ask if facial perception can also be biased toward higher spatial frequency content by FFAd.

Experiment 1: FFAd and Facial Coding

Methods. Ethical approval for all experiments was obtained from the University of Queensland Ethics Committee, and were in accordance with the Declaration of Helsinki. Before the experiment began, participants read an instruction screen and were informed that they could withdraw from the experiment at any time without penalty. They indicated their consent to participate by clicking, to indicate that they had read and understood the instructions.

There were 10 participants (four male), of whom 3 were authors. Others were naïve as to the experimental purpose. All had normal or corrected-to-normal visual acuity. Stimuli were displayed on a Samsung SyncMaster 950p+ monitor at a resolution of 1,024 × 768 updated at 75 Hz. Stimuli were viewed from 57 cm in a darkened room with the participant's head placed in a chin rest. The dynamic noise adapting pattern subtended 10 degrees of visual angle (dva) in width and 5 dva in height, with individual elements subtending 0.42 dva in width and height.

Exemplar gray-scale male and female faces were generated by averaging 10 celebrity facial images of either gender using the Face Mixer function in Abrosoft FantaMorph. Image-based low-pass and band-pass filtered versions of these were generated, using a Gaussian filter with a σ of 0.04 for low-pass (see leftmost images in Fig. 1*A*) and a σ of 0.14 centered on 0.3 image cycles for band-pass filtering (Fig. 1*A*, rightmost images). Two arrays of 11 test images were generated, with low-pass image contrast changing linearly from 1 to 0 and band-pass image contrast changing from 0 to 1. One array of test images was generated from a low-pass female and a band-pass male exemplar image and another from a low-pass male and a band-pass female image. In both cases, the average gray scale value of all array images was equated. Test images subtended 4.4 dva in width and height and were centered in the middle of the display.

During a block of trials, each of the 11 test images in each of the two image arrays was presented eight times, for a total of 176 individual trials, all completed in random order. After each test presentation, participants categorized the face as having looked masculine or feminine. A small (0.2 dva) red fixation point was present throughout testing. In different experimental blocks, the fixation point was centered on either the middle of the display (0-dva tests) or 6 dva to the left of the display center (6-dva tests). Each participant completed four blocks with a baseline and then an adaptation block of trials completed for each test eccentricity. Order (0-dva then 6-dva tests, or 6-dva then 0-dva tests) was counterbalanced across participants. As the task was a subjective gender categorization (male/female), we were unconcerned about practice effects, so for each test, eccentricity baseline blocks were completed before adaptation blocks.

During adaptation blocks, each trial began with the presentation of a dynamic noise pattern, for 10 s on the 1st and 35th trials, and for 5 s on other trials. These were updated at the monitor refresh rate and were centered on the display center. After the dynamic noise pattern disappeared, there was a 0.25-s interstimulus interval before a 0.25-s test presentation. The next trial began 0.95–1.95 s after the participant had indicated a response (precise delay determined at random on a trial-by-trial basis). Baseline blocks were quicker than adaptation blocks, as the adaptation sequence was omitted on each trial. The test portions of these blocks of trials were identical to adaptation blocks of trials (Fig. 1*B*, graphic description of presentation protocol).

Each block of trials provided two distributions describing perceived gender as a function of the ratio of low-pass to band-pass image content. A logistic function was fitted to each and the 50% point taken as an estimate of the gender category boundary for that array of test images. These were averaged for each participant, providing a single individual estimate.

Results. A two-way repeated measures analysis of variance was conducted, with adaptive state (baseline or adapted) and test eccentricity (0 or 6) as within subject factors. This revealed significant main effects of adaptation ($F_{1,9} = 8.55$, $P = 0.017$, $\eta_p^2 = 0.49$) and test eccentricity ($F_{1,9} = 30.99$, $P < 0.001$, $\eta_p^2 = 0.78$; Fig. 1*C*). Follow up *t* tests revealed that these effects were due to gender perception being biased toward lower spatial frequency content for 6-dva tests (average low- to band-pass image content ratio at face category boundary M 0.81 SD 0.12) relative to 0-dva tests (M 0.59 SD 0.11; $t_9 = 5.54$, $P < 0.001$), and to gender perception being biased toward higher spatial frequencies postflicker adaptation (M 0.68 SD 0.10)

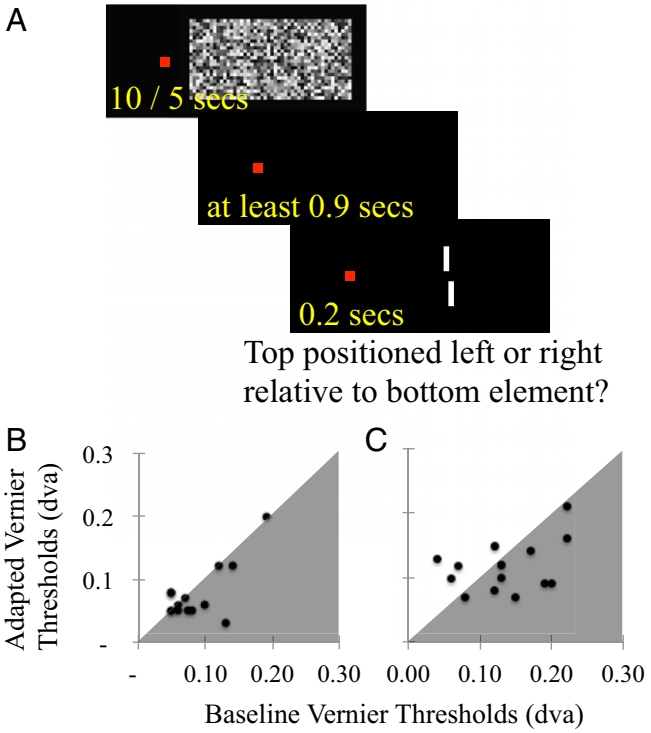

Fig. 2. (*A*) Depiction of a trial sequence during a block of adaptation trials in experiment 2. On each trial, the participant viewed dynamic noise (60 Hz) centered to the right of fixation, for 10 s on the first trial, and for 5 s on all subsequent trials. Then there was a 400-ms interstimulus interval, before fixation monitoring commenced. Test presentations, lasting 200 ms, were triggered once 500 ms of stable fixation had been achieved—so tests followed adaptors by at least 900 ms. (*B* and *C*) Scatterplots of individual adapted (vertical axes) and unadapted baseline (horizontal axes) vernier thresholds from experiment 3. Data are plotted separately for average test eccentricities of 10 (*B*) and 20 (*C*) dva. Data points in gray shaded regions indicate improved vernier acuity post-FFAd; points in unshaded regions indicate poorer acuity.

relative to baseline (M 0.72 SD 0.09, $t_9 = 3.14$, $P = 0.012$). There was no evidence of an interaction between adaptive state and test eccentricity ($F_{1,9} = 0.07$, $P = 0.79$, $\eta_p^2 = 0.01$).

Discussion. In experiment 1 we showed that FFAd can have a perceptual impact on what is perhaps the most important biological form we experience—the human face. These data suggest that visual mechanisms subject to FFAd disproportionately contribute to encoding low spatial frequency content, and that these can add "blur" when the visual system synthesizes signals from different spatial scales to create a coherent impression of form. In experiment 2, we ask if the transient mitigation of this contribution can be advantageous—we ask if FFAd can transiently improve the acuity of spatial vision.

Experiment 2: FFAd and Positional Sensitivity

Methods. There were 16 participants (six male), of whom 3 were authors. Others were naïve as to the experimental purpose. All had normal or corrected-to-normal visual acuity. Experimental stimuli were generated using Matlab R2012b software (MathWorks) in conjunction with the Psychophysics Toolbox (21, 22) and were displayed on a Dell 2714t liquid crystal display at a resolution of 1,920 × 1,080 pixels updated at 60 Hz. Stimuli were viewed from 60 cm in a darkened room, with the participant's head secured by a chin rest. Responses were recorded via mouse button presses. Fixation was monitored via a LiveTrack Fixation monitor from Cambridge Research Systems.

On each trial a small red square, subtending 0.2 dva at the retina, served as a fixation point. In different blocks of trials, the fixation square was positioned either 10 or 20 dva to the left of the display center, which contained two vertically separated (1 dva gap) white bars, each subtending 1 dva in height and 0.1 dva in width (Fig. 1, graphic). During a block of trials the horizontal separation of the vernier elements was adjusted according to an interleaved one up, two down staircase procedure, wherein an incorrect response resulted in an increase in separation (0.025) for that staircase, and two successive correct responses in a decrease in separation (0.025). This concentrated sampling at a test magnitude resulting in ~70% correct task performance. One of the two staircases was instigated at a maximal separation (0.25 dva), the other at a minimal separation (0.025 dva). These maximal and minimal test values were enforced throughout testing.

Direction of test offset (top element displaced left/bottom right, or top element offset right/bottom left) was determined at random on a trial-by-trial basis, and participants were required to indicate the position of the top element relative to the bottom by pressing one of two mouse buttons. On average, the vernier stimulus was positioned in the center of the display, but this was manipulated during a block of trials (ranging 4.5 dva left to 4.5 dva right) according to a method of constant stimuli. This was done to ensure participants attended to both test elements on a trial-by-trial basis and could not complete the task by attending to just one and judging its position relative to the display center. A block of trials consisted of 70 individual test presentations, 35 from each staircase, all completed in random order. A logistic function was fit to data resulting from each block of trials, and the distance between the 50% and 70% points on the fitted function was taken as an estimate of the participants' threshold separation for correct position judgments in that condition.

During adaptation blocks, each trial began with the presentation of a dynamic noise pattern, subtending 18 dva in width and 9 dva in height, with individual elements subtending 0.75 dva in width and height. This dynamic noise pattern was presented for 10 s on the 1st and 35th trials and for 5 s on all other trials. The white noise pattern was updated at the monitor refresh rate (60 Hz) and was centered on the display center. After the noise pattern disappeared, there was a 0.4-s delay before onset of fixation monitoring. Test presentations were triggered once steady gaze at the fixation had persisted for 0.5 s. Fixation coordinates were recorded via the LiveTrack Fixation monitor throughout this period until immediately after each test presentation. If an eye movement occurred (a gaze drift >0.15 dva in any direction), trial data were discarded and a new test stimulus was presented, with vernier direction rerandomized to avoid practice effects. The next trial began 0.5 s after the participant had indicated a response. The test portion of baseline blocks was similar to adaptation blocks, but the adaptation sequence was omitted on each trial. There was also a 0.9-s delay between responses and the beginning of the next trial. In each case, blocks persisted until 75 trials were successfully completed (Fig. 2*A*, graphic).

Each participant completed four blocks of trials, one baseline and one adaptation block of trials for tests centered (on average) at both 10 and 20 dva from fixation. Completion of blocks of trials for each test eccentricity was grouped, with order (baseline then adaptation, or adaptation then baseline) counterbalanced across participants. The order in which the two test eccentricities were completed (10 dva then 20 dva, or 20 dva then 10 dva) was also counterbalanced across participants. This ensured that practice effects did not contaminate our adaptation measures. A minimal time of 30 min in between successive blocks of trials was enforced.

Results. Inspection of the data revealed no outliers, so all data (Fig. 2 *B* and *C*) were subjected to a two-way repeated measures analysis of variance, with adaptive state (baseline or adapted) and

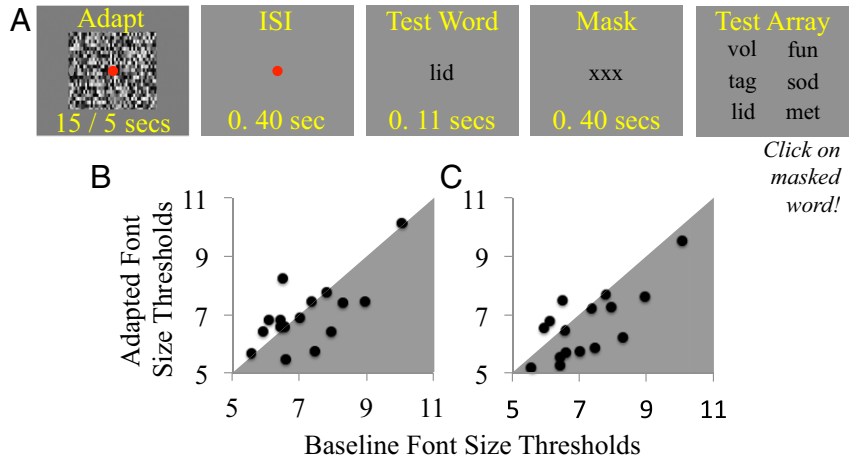

Fig. 3. (*A*) Depiction of a trial sequence during an adaptation trial of experiment 3. (*B* and *C*) Scatterplots of individual adapted (vertical axes) and unadapted baseline (horizontal axes) font-size thresholds from experiment 4. Data are plotted separately for SFAd (*B*) and FFAd (*C*). Data points falling in gray shaded regions indicate improved sensitivity postadaptation; points in unshaded regions indicate poorer sensitivity.

test eccentricity (10 or 20) as within subject factors. This analysis revealed significant main effects of adaptation ($F_{1,14} = 6.4$, $P = 0.024$, $\eta_p^2 = 0.31$) and test eccentricity ($F_{1,14} = 23.4$, $P < 0.001$, $\eta_p^2 = 0.57$). Follow up t tests showed that the effect of adaptation was due to enhanced vernier acuity postadaptation (M 0.09 SD 0.03) relative to baseline (M 0.11 SD 0.04; $t_{14} = 2.53$, $P = 0.024$), and that the effect of eccentricity reflected poorer acuity for 20 dva tests (M 0.13 SD 0.04) relative to 10 dva tests (M 0.08 SD 0.04, $t_{13} = 4.84$, $P < 0.001$). There was no evidence of an interaction between adaptive state and test eccentricity ($F_{1,14} = 1.62$, $P = 0.22$, $\eta_p^2 = 0.10$).

Discussion. Experiment 2 results show that increasing test eccentricity and FFAd impact spatial perception in opposite ways. Increasing test eccentricity reduced the acuity of spatial perception, whereas FFAd enhanced spatial acuity. The former observation was expected, as human vision prioritizes processing as a function of distance from fixation (23–25). The latter observation is novel, but is consistent with our motivating premise—that vernier elements are usually encoded by multiple relatively independent processes with differing spatial resolutions, and that FFAd can transiently reduce the influence of poor spatial resolution processes, thereby enhancing the acuity of spatial vision.

Although vernier acuity is a standard measure of visual acuity, its real-world relevance is perhaps obscure. In experiment 3, we therefore decided to see if FFAd could advantage a real-world task—reading fine print.

Experiment 3: FFAd and Fine Print Acuity

Methods. There were 16 participants (10 male), of whom 2 were authors. Others were naïve as to the experimental purpose. All had normal or corrected-to-normal visual acuity. Experimental stimuli were generated using Matlab R2012b software (MathWorks) in conjunction with the Psychophysics Toolbox (21, 22) and were displayed on a 19-inch Samsung SyncMaster 950p+ at a resolution of 1,280 × 1,024 pixels updated at 75 Hz. Stimuli were viewed from 57 cm in ambient lighting with the participant's chin resting on a chin rest. The display background was gray [Commission Internationale d'Éclairage (CIE) 1931 chromaticity chart × 0.31 y 0.35 Y 26]. Responses were recorded via mouse movements and button presses.

A small red square, subtending 0.2 dva^2 at the retina and centered on the display, served as a fixation point during adaptation periods, and for 0.4 s before test word presentations (Fig. 3*A*, graphic). Adaptors consisted of 8 × 5 dva dynamic noise patterns (individual elements 0.03 dva^2), in different blocks of trials they were either updated at the monitor refresh rate (FFAd) or at 0.67 Hz to create slow flicker adaptation (SFAd). After adaptation, there was a 400-ms interstimulus interval (ISI), followed by a 107-ms test word presentation, then a 400-ms mask ("XXX" in the same font size as the test word). A test array of six clearly legible words was then presented, and participants tried to click on the masked test word—conceptually a six alternative forced choice match-to-sample task, but in practice perhaps a more binary task, as performance was limited by being able to resolve text. The test portion of trials in unadapted baseline blocks of trials was identical to adaptation blocks, but adaptation procedures were omitted. Words were three letters long, selected from the On-Line Orthographic Database on the basis of constrained trigram statistics (www.neuro.mcw.edu/mcword/). All text was black (Fig. 3*A*, graphic).

During a block of trials, test word font size was adjusted according to interleaved one up, two down staircase procedures, wherein incorrect responses resulted in an increase in font size, and two successive correct responses for a given staircase in a decrease. One of the two staircases began at a maximal font size (12: maximal letter height ~0.25 dva), the other at a minimal font size (3: maximal letter height ~0.1 dva). These maximal and minimal font sizes were enforced during testing, so mistaken incorrect responses would not result in larger font sizes being sampled, and correct guessing would not result in smaller font sizes being sampled. A block of trials persisted for 90 individual trials (45 trials for each staircase, interleaved in random order). Each participant completed three blocks of trials. They first completed the adaptation block of trials, with order (FFAd then SFAd, or SFAd then FFAd) counterbalanced across participants. All participants completed an unadapted baseline block of trials last, so task practice could not generate a false impression of an adaptation benefit.

Results. Logistic functions were fit to data describing successful test word matching as a function of font size from each block of trials, and 79% points were taken as font size threshold estimates. Individual threshold estimates are depicted in Fig. 3 *B* and *C*.

Individual aftereffect scores, for SFAd and FFAd, were calculated by determining differences between adapted and unadapted baseline threshold estimates. Analyses of these scores revealed that SFAd had had no discernible impact on text acuity [M 0.21 SD 0.96, single sample $t_{15} = 0.86$, $P = 0.403$, 95% confidence intervals (CIs) −0.31 to +0.72; Fig. 3*B*], whereas FFAd improved text acuity (M 0.57 SD 0.92, $t_{15} = 2.48$, $P = 0.025$, 95% CIs +0.08 to +1.06; Fig. 3*C*).

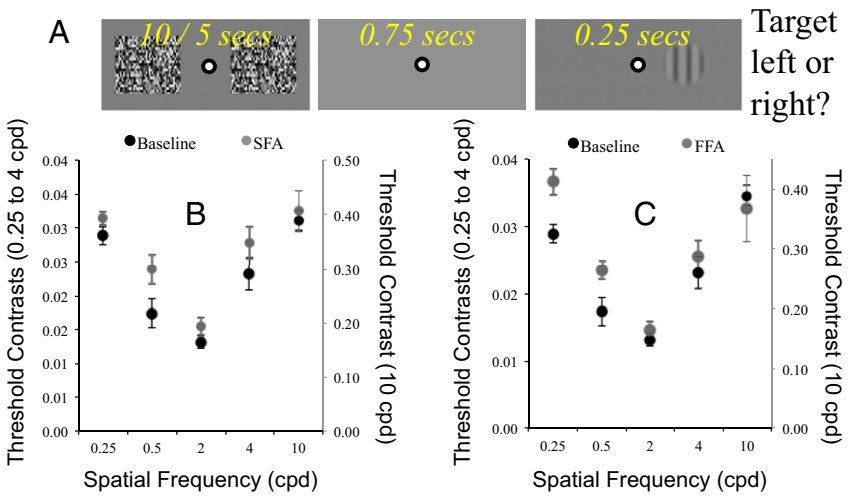

Fig. 4. (*A*) Depiction of a trial sequence during a block of adaptation trials in experiment 4. (*B*) Contrast thresholds, averaged across participants, as a function of test spatial frequency at baseline (black) and post-SFAd (gray). (*C*) As for *B*, for baseline (black) and FFAd (gray). Error bars denote ±1 SEM.

Discussion. Thus far, we have shown that FFAd can enhance the acuity of spatial vision (experiments 2 and 3), and that FFAd can bias face perception in favor of band-pass, over low-pass spatial frequency content (experiment 1). In combination, these results are consistent with FFAd selectively reducing the contribution of magno fed mechanisms that encode the lower spatial frequency content of spatial form. In experiment 4, we assess this possibility more directly by determining whether FFAd selectively reduces sensitivity to low-pass spatial frequencies.

Experiment 4: Flicker Adaptation and Contrast Sensitivity

Methods. In experiment 4, there were 10 adult participants (six male), of whom 2 were authors. Others were naïve as to the experimental purpose. All had normal or corrected-to-normal visual acuity. Stimuli were generated using a ViSaGe stimulus generator from Cambridge Research Systems, driven by Matlab 7.5 software, and displayed on a γ-corrected Samsung Syncmaster 1100p monitor (resolution 1,280 × 1,024, refresh rate 120 Hz), viewed from 57 cm in a dark room with the participant's chin on a chin rest. Responses were recorded via mouse button presses.

A small black and white bull's-eye configuration, subtending 0.2 dva at the retina, was positioned in the display center to serve as the fixation point throughout the experiment. The display background was gray (CIE × 0.281 y 0.298 Y 58 candela/m^2). During adaptation blocks, each trial began with the presentation of two dynamic noise patterns, each subtending 8 dva^2 (individual elements 0.04 dva^2) and centered 10 dva to the left and right of fixation. Noise patterns were either updated at the monitor refresh rate (120 Hz, FFAd) or at 0.8 Hz to induce SFAd. Noise patterns were presented for 15 s on the first and the midtrial of a block, and for 5 s on all other trials. When noise patterns disappeared, there was a 0.75-s interstimulus interval before a 0.25-s test presentation. The participants' task was to report on which side of fixation the target had been presented. Feedback was provided—a rising tone for correct responses, a descending tone for incorrect responses. The next trial began 0.25 s after the participant had received feedback. Baseline blocks of trials were more rapid, as these omitted the adaptation sequence on each trial (Fig. 4*A*, graphic).

Test stimuli consisted of a single vertical Gabor pattern, subtending 4 dva^2, spatial constant 0.67 dva, centered 10 dva to the left or right of fixation (determined at random on a trial-by-trial basis). Test spatial frequency was 0.25, 0.5, 2, 4, or 10 cycles per degree (cpd) of visual angle.

There were two trial block types, concentrated and comprehensive. In concentrated blocks only the highest (10 cpd) and lowest (0.25 cpd) spatial frequencies were sampled. During comprehensive blocks, all test spatial frequencies were sampled. In each case, trials were blocked—all trials for a particular spatial frequency were sampled together. Test spatial frequency order was randomized for each block of trials.

Each participant completed both a concentrated and a comprehensive block of trials for each experimental condition, and data were collated across these two blocks before analysis. Half the participants completed concentrated blocks first, others comprehensive. In each case, participants first completed a baseline block of trials, then the two adaptation blocks of trials in sequence—with adaptation condition (SFAd/FFAd) order counterbalanced across participants.

During each block of trials, test contrast was adjusted according to a one up, two down staircase procedure for each test spatial frequency, wherein an incorrect response resulted in an increase in test contrast, and two successive correct responses resulted in a decrease in contrast. This staircase concentrated sampling at test contrasts, resulting in ∼70% successful target localization. Each staircase was instigated at a clearly suprathreshold level. Concentrated blocks of trials persisted for 160 individual trials (80 for each of two test spatial frequencies), whereas comprehensive blocks of trials persisted for 200 individual trials (40 trials for each of five test spatial frequencies).

Results. Logistic functions were fit to proportion correct data for each test spatial frequency in each test condition for each participant, and 75% points were taken as contrast detection threshold estimates. The mean of these estimates, averaged across participants, is plotted as a function of test spatial frequency in Fig. 4 *B* (SFAd) and *C* (FFAd). Appraisal of these data reveals that FFAd worsened thresholds selectively at lower spatial frequencies (0.25 and 0.5), with no obvious change at the highest spatial frequency (10). We conducted paired *t* tests to confirm this general pattern. For the lowest spatial frequency tested (0.25 cpd) thresholds were worse after FFAd (M 0.037 SD 0.006) relative to baseline (M 0.029 SD 0.004; $t_9 = 3.2$, $P = 0.011$), whereas SFAd induced no difference (M 0.031 SD 0.003; $t_9 = 1.48$, $P = 0.174$). For the highest spatial frequency tested (10 cpd) there was no change in thresholds from baseline (M 0.39 SD 0.02) after either FFAd (M 0.37 SD 0.06; $t_9 = 0.4$, $P = 0.669$) or SFAd (M 0.41 SD 0.04; $t_9 = 0.72$, $P = 0.49$).

General Discussion

Our data show that human form perception can transiently be sharpened by FFAd. We have found that FFAd can temporarily (*i*) bias facial coding in favor of high spatial frequency content (experiment 1), (*ii*) heighten spatial acuities (experiments 2 and 3), and (*iii*) selectively depress spatial contrast sensitivity at low spatial frequencies (experiment 4).

To be clear, we are not proposing that FFAd works by directly enhancing the responses of "parvo"-fed mechanisms sensitive to high spatial frequencies. Rather, we believe human vision synthesizes form signals across a range of spatial frequency-tuned mechanisms, and that FFAd works by selectively reducing the contribution of "magno"-fed channels that encode coarse spatial resolutions. Attenuating this contribution results in perceptual sharpening, as these channels add blur (low spatial frequency content) to perception. Our results would thus be akin to the well-known demonstration that the ability to recognize a pixelated face can be improved by removing uninformative high spatial frequency content—by blurring the image by squinting. In both cases, perception is improved by attenuating information harmful to the task at hand—in this case, blurry low spatial frequency content when attempting to make fine spatial judgments and in the other case, uninformative high spatial frequency content that obscures a person's identity.

It is well established that human spatial vision can be sharpened by adaptation. Prolonged exposure to images apparently (26) or actually (27–29) containing lower spatial frequency content can make other images appear sharpened. We do not think this can account for our data. The SFAd and FFAd conditions of experiments 3 and 4 were matched in terms of their spatial characteristics, and in both experiments, FFAd biased coding in favor of higher spatial frequency content, and SFAd had no discernible impact. We are thus confident that the efficacy of FFAd across all our experiments was due to adaptation to stimulus dynamics, rather than to spatial characteristics.

One implication of our data is that human vision is not mediated by mechanisms that independently encode for stimulus dynamics and spatial form (1–3). The distinction between dynamics and form had already been challenged by physiological (4–6) and behavioral (7) observations. Our data provide a further challenge—they show that adapting to stimulus dynamics can sharpen spatial perception, revealing an influence of mechanisms with joint spatial (low) and temporal (high) frequency tunings. This does not imply an absence of specialization. Rather, it would seem that spatial vision is shaped by relatively independent, specialized, mechanisms that can be differentially adapted.

Another implication is that the acuity of spatial vision is not optimized when unadapted. At face value, this suggestion might seem odd. Why would the visual system be suboptimal for performing spatial judgments in an unadapted state? An answer might rest in the properties of the images we encounter in daily life. Analyses of images depicting natural scenes reveal that most image variance occurs at coarse spatial scales. There is progressively less variance at finer spatial scales, and the drop off is approximately linear if plotted on a log scale—so natural images can be said to conform to a $1/f$ amplitude spectrum, where f reflects spatial scale (15, 30, 31). In normal circumstances, it might therefore be advantageous to prioritize analyses of lower over higher spatial frequencies. Moreover, it might be inaccurate to conceptualize baseline conditions as unadapted. Rather, these can be conceived of as adapted to natural image statistics, and hence optimized for encoding the visual characteristics of everyday experience.

Our data speak directly to the encoding of briefly seen spatial forms. This is not entirely irrelevant for daily life, as when we glance about the world, rapidly shifting gaze from one point to another, the processes we have identified will likely be at play. The influence of FFAd would, however, likely diminish with more protracted viewing.

Most of the tasks we complete on a daily basis, like recognizing human faces, must depend primarily on information encoded at a relatively coarse spatial scale. From this perspective, it is possibly unsurprising that human form perception typically disproportionately reflects image content at a coarse spatial scale. That FFAd can shift this balance toward finer spatial frequencies is consistent with the premise that mechanisms with a high temporal resolution usually contribute a blurred signal to form perception, and weakening this contribution can transiently sharpen that vision. Accordingly, next time you wish to read the fine print on a form (a difficult task demanding a fine spatial acuity), and you don't have a magnifying glass to hand—you might be well advised to first view a flickering field of dynamic noise!

ACKNOWLEDGMENTS. This research was supported by an Australian Research Council Discovery Future Fellowship (FT130100605) and Discovery Project Grant (DP140100494) to D.H.A.

1. Livingstone MS, Hubel DH (1987) Psychophysical evidence for separate channels for the perception of form, color, movement, and depth. *J Neurosci* 7(11):3416–3468.
2. Ungerleider LG, Mishkin M (1982) Two cortical visual systems. *Analysis of Visual Behavior*, eds Ingle DJ, Goodale MA, Mansfield RJW (MIT Press, Cambridge, MA), pp 549–586.
3. Zeki S (1983) Colour coding in the cerebral cortex: The reaction of cells in monkey visual cortex to wavelengths and colours. *Neuroscience* 9(4):741–765.
4. Lennie P (1998) Single units and visual cortical organization. *Perception* 27(8): 889–935.
5. Felleman DJ, Van Essen DC (1987) Receptive field properties of neurons in area V3 of macaque monkey extrastriate cortex. *J Neurophysiol* 57(4):889–920.
6. Gegenfurtner KR, Kiper DC, Levitt JB (1997) Functional properties of neurons in macaque area V3. *J Neurophysiol* 77(4):1906–1923.
7. Nishida S (2004) Motion-based analysis of spatial patterns by the human visual system. *Curr Biol* 14(10):830–839.
8. Burr D (1980) Motion smear. *Nature* 284(5752):164–165.
9. Chen S, Bedell HE, Oğmen H (1995) A target in real motion appears blurred in the absence of other proximal moving targets. *Vision Res* 35(16):2315–2328.
10. Gegenfurtner KR, Brown JE, Rieger J (1997) Interpolation processes in the perception of real and illusory contours. *Perception* 26(11):1445–1458.
11. Burr D, Ross J (1982) Contrast sensitivity at high velocities. *Vision Res* 22(4):479–484.
12. Baizer JS, Ungerleider LG, Desimone R (1991) Organization of visual inputs to the inferior temporal and posterior parietal cortex in macaques. *J Neurosci* 11(1):168–190.
13. Cao D, Shevell SK (2005) Chromatic assimilation: Spread light or neural mechanism? *Vision Res* 45(8):1031–1045.
14. DeValois R, DeValois K (1975) Neural coding of color. *Handbook of Perception V*, eds Carterette EC, Friedman MP (Academic, New York), pp 117–166.
15. Geisler WS, Albrecht DG, Crane AM, Stern L (2001) Motion direction signals in the primary visual cortex of cat and monkey. *Vis Neurosci* 18(4):501–516.
16. Geisler WS (1999) Motion streaks provide a spatial code for motion direction. *Nature* 400(6739):65–69.
17. Arnold DH, Erskine HE, Roseboom W, Wallis TS (2010) Spatiotemporal rivalry: A perceptual conflict involving illusory moving and static forms. *Psychol Sci* 21(5):692–699.
18. Cass J, Alais D (2006) Evidence for two interacting temporal channels in human visual processing. *Vision Res* 46(18):2859–2868.
19. Grindley GC, Townsend V (1965) Binocular masking induced by a moving object. *Q J Exp Psychol* 17:97–109.
20. Schyns PG, Oliva A (1999) Dr. Angry and Mr. Smile: When categorization flexibly modifies the perception of faces in rapid visual presentations. *Cognition* 69(3):243–265.
21. Brainard DH (1997) The psychophysics toolbox. *Spat Vis* 10(4):433–436.
22. Pelli DG (1997) The VideoToolbox software for visual psychophysics: Transforming numbers into movies. *Spat Vis* 10(4):437–442.
23. Daniel PM, Whitteridge D (1961) The representation of the visual field on the cerebral cortex in monkeys. *J Physiol* 159:203–221.
24. Johnston A, Wright MJ (1983) Visual motion and cortical velocity. *Nature* 304(5925): 436–438.
25. Rovamo J, Virsu V (1979) An estimation and application of the human cortical magnification factor. *Exp Brain Res* 37(3):495–510.
26. Parker A (1981) Shifts in perceived periodicity induced by temporal modulation and their influence on the spatial frequency tuning of two aftereffects. *Vision Res* 21(12): 1739–1747.
27. Blakemore C, Sutton P (1969) Size adaptation: A new aftereffect. *Science* 166(3902): 245–247.
28. Elliott SL, Georgeson MA, Webster MA (2011) Response normalization and blur adaptation: Data and multi-scale model. *J Vis* 11(2):7.
29. Webster MA, Georgeson MA, Webster SM (2002) Neural adjustments to image blur. *Nat Neurosci* 5(9):839–840.
30. Maloney LT (1986) Evaluation of linear models of surface spectral reflectance with small numbers of parameters. *J Opt Soc Am A* 3(10):1673–1683.
31. Field DJ (1987) Relations between the statistics of natural images and the response properties of cortical cells. *J Opt Soc Am A* 4(12):2379–2394.